Quantum Inf Process (2016) 15:4911–4925
DOI 10.1007/s11128-016-1401-1

Leggett–Garg inequalities for a quantum top affected by classical noise

Jerzy Dajka[1,2] · **Marcin Łobejko**[1,2] · **Jerzy Łuczka**[1,2]

Received: 4 April 2016 / Accepted: 21 July 2016 / Published online: 1 August 2016

Abstract The violation of the Leggett–Garg inequality is studied for a quantum top (with angular momentum J_z of integer or half-integer size), being driven by classical Gaussian white noise. The form of a longitudinal (J_z) or a transverse (J_x) coupling of noise to the angular momentum affects both (i) to what extent the Leggett–Garg inequality is violated and (ii) how this violation is influenced by the size j of the spinning top and direction of a coupling (transverse or longitudinal). We introduce j-independent method, using two- dimensional invariant subspace of the system Hilbert space, which allows us to find out strict analytical solution for a noise-free system and with longitudinal coupling and to extract from the whole dynamics effects purely induced by a noise. It is demonstrated that in the semi-classical limit of a large angular momentum j and for the transverse coupling, the Leggett–Garg inequalities become more strongly violated as compared to the deep quantum regime of small j.

Keywords Leggett–Garg inequalities · Temporal quantum correlations · Quantum open systems · Dissipative dynamics · Classical noise

✉ Marcin Łobejko
mlobejko@us.edu.pl

Jerzy Dajka
jerzy.dajka@us.edu.pl

Jerzy Łuczka
jerzy.luczka@us.edu.pl

1 Institute of Physics, University of Silesia, Katowice, Poland

2 Silesian Center for Education and Interdisciplinary Research, University of Silesia, Chorzow, Poland

1 Introduction

There are various properties of quantum systems which are worth to be designed and controlled. Quantum entanglement [18] (and other types of *spatial* correlations [29]), a useful resource for quantum information, is among these properties of time-evolving quantum systems which attract considerable attention. Presence of entanglement can be detected [15] by the violation of various forms of Bell inequalities [5]. Recent studies on quantum correlations *in time* show that such correlations are no less interesting as these in space [12]. Non-classical time correlations between outcomes of measurements realized at different time instants are indicated by the violation of the Leggett–Garg inequalities (LGIs) [21]. The Leggett–Garg and the Bell scenarios can formally be unified [26]; however, interpretation of what is actually tested by LGIs seems to be still unclear [27]. In Ref. [12], there is an up-to-date review of both basic theoretical and experimental achievements related to the LGI.

The simplest form of the LGI reads [12]

$$K_3 = C_{21} + C_{32} - C_{31} \leq 1. \tag{1}$$

The correlator $K_3 \equiv K_3(t)$ is a combination of three time correlation functions given by an expected value of an anti-commutator [12] $C_{ji} = \frac{1}{2}\langle\{Q(t_j), Q(t_i)\}\rangle$ of a dichotomous observable $Q(t)$ in the Heisenberg picture with corresponding measurement values $q(t) = \pm 1$ at three successive time instants $t_1 < t_2 < t_3$. Due to the existence of superposition states, quantum mechanics should violate the above inequality. Experimental testing of LGIs and search for their possible violation are subtle problems due to required non-invasiveness of measurement of the quantity Q [12] and 'macroscopicity' of quantum states. The LGIs are interesting by their own also in microscopic systems [6] so the second requirement is often abandoned. There are also certain conceptual difficulties related to the problem of the 'clumsiness loophole' [12]. In order to avoid confusion, we simply claim that the violation of the LGI in (1) is a hallmark of the violation of the *Leggett–Garg realism* in the considered system. In such a way, we attempt to encapsulate all the fundamental problems related to a proper interpretation of the violation of the inequality (1), cf. Ref. [27].

Calculation of the correlation functions C_{ji} for the case of strictly Markovian evolution of a quantum system (either closed or open) is simplified by negligibility of entanglement between the system and its environment [11]. For any quantum system prepared at time t_0 in a state $\rho(t_0)$ evolving according to Markovian and continuous time dynamical semigroup $\rho(t) = \Lambda(t - t_0)\rho(t_0)$, the correlation functions in Eq. (1) can be expressed by the relation in the Schrodinger picture [6]:

$$C_{ji} = \sum_{l,m} q_m q_l \mathrm{Tr}\left\{\Pi_m \Lambda(t_j - t_i)[\Pi_l \Lambda(t_i)\rho(0)\Pi_l]\right\}, \tag{2}$$

where Π_l are projector operators representing the measurement of the dichotomous quantity $Q = Q(0)$ with the measurement output either $q_l = +1$ or $q_l = -1$.

The design of appropriate features of evolving quantum systems is a subject of the quantum control theory [8]. For quantum systems, an open-loop control is conceptually

simpler than a closed loop one as it does not demand feedback with respect to an output of a measurement performed on a quantum system [34]. There are various types of open-loop driving. The simplest is a classical field (e.g., magnetic or electric) which introduces a time- dependent component to a Hamiltonian of the quantum system. The most complex is a quantum field such as n-mode bosonic field typical for quantum optical problems [34]. Somewhere in between is a classical stochastic driving (stochastic control [16]) which can be considered either as a classical field with certain degree of randomness or as a suitable stochastic limit of a quantum driving [1]. There is a deep relation between dynamic properties of evolving systems and their symmetries [8]. One of the best studied symmetries is related to rotation of the system and its angular momentum [3]. Quantum systems described by Hamiltonians built by angular momentum operators, either integer or half-integer, are called quantum tops and are widely studied in various branches of physics starting from mathematical physics [31] via quantum chaos [17] up to quantum networks [25]. As the quantum tops have a well-defined classical limit [17], they are particularly important for studies of quantum properties in a semi-classical limit. For instance, one can investigate how quantum entanglement is maintained when a system or its part [7,9] becomes 'more classical' and compare results with other approaches to a classical limit of quantum systems [10,13,20].

In this work, we study a quantum top driven by Gaussian white noise and analyze the noise impact on the violation of the LGI. We consider two ways how the noise source couples to the top, each leading to quantitatively different behavior of the correlator K_3. The external noise weakens the violation of the LG inequality, but this effect is less significant in the semi-classical limit of the large top. We show that, counterintuitively, in the semi-classical regime, the Leggett–Garg realism is more likely to be broken than in the very quantum regime.

The paper is organized as follows: In Sect. 2, we describe a model of the quantum top driven by Gaussian white noise and discuss an equivalence of its evolution with a suitably constructed Lindblad quantum dynamical semigroup. In Sect. 3, we present and discuss properties of the function K_3 for the noise-assisted system. We compare this result to a purely deterministic, noiseless evolution. Next, before summarizing the work in Sect. 4, we conjecture that the properties of the function K_3 originate from the fact that in the semi-classical limit the noise-driven and noiseless quantum tops are less distinguishable.

2 Methods

2.1 Noise-assisted top

Quantum tops are studied in different contexts in various branches of physics. Semi-classical methods related to the field of quantum chaos [17] are probably most widely known. Here we consider a simple model of an angular momentum $\mathbf{J} = (J_x, J_y, J_z), [J_i, J_j] = i\hbar\epsilon_{ijk}J_k$, where ϵ_{ijk} is the completely antisymmetric Levi-Civitá symbol. The eigenvalues Λ_j of the operator $\mathbf{J}^2$ are $\Lambda_j = \hbar^2 j(j+1)$, $j \in \{0, 1/2, 1, 3/2, 2, \ldots\}$. The time evolution of the top is governed by the Hamiltonian

$$H = \hbar\omega_0 \frac{J_z}{j} + \hbar\lambda_0 \tilde{\xi}(t) \frac{V}{j}, \quad V = J_z \quad \text{or} \quad V = J_x, \tag{3}$$

where $\tilde{\xi}(t)$ is an external random driving (noise). The first term describes a precession around the z axis with the scaled angular frequency ω_0/j. The second term can be interpreted as random kicks around the z axis for $V = J_z$ or around the x axis for $V = J_x$ by random angles proportional to the coupling strength λ_0/j and the square root of the intensity D_0 of noise (which is defined by its correlation function, see below). We use such scaling because in the limit $j \to \infty$ mean values of three quantities

$$X = \frac{\langle J_x \rangle}{j}, \quad Y = \frac{\langle J_y \rangle}{j}, \quad Z = \frac{\langle J_z \rangle}{j}, \tag{4}$$

become [33]

$$(X, Y, Z) = (\sin\theta\cos\phi, \sin\theta\sin\phi, \cos\theta), \tag{5}$$

where θ is the polar angle and ϕ is the azimuthal angle. Therefore, (X, Y, Z) represents a point on the Bloch sphere with radius $R = 1$. For large $j \gg 1$, semi-classical behavior should be uncovered.

We restrict our consideration to a linear coupling of the system with noise and two possible choices: either $V = J_z$ or $V = J_x$. The coupling to J_y is equivalent to the coupling to J_x and therefore is not considered. The coupling $V = J_z$ corresponds to a simplest 'dephasing-like' coupling [4,22], whereas the second coupling $V = J_x$ could describe tunneling effects in some multistable systems. As we show below, these two cases result in significantly different behaviors of the corresponding function K_3.

The classical and real-valued stochastic driving $\tilde{\xi}(t)$ is modeled by zero-mean δ-correlated Gaussian white noise,

$$\langle \tilde{\xi}(t) \rangle = 0, \tag{6}$$

$$\langle \tilde{\xi}(t)\tilde{\xi}(s) \rangle = 2D_0\delta(t-s), \tag{7}$$

where $\langle\cdot\rangle$ means the averaging over all realizations of the stochastic process $\tilde{\xi}(t)$ [14] and the parameter D_0 is the intensity of noise. We should remember that the characteristic time of white noise, i.e., its correlation time, is zero, and therefore, it does not introduce a new time scale into the system.

For each realization of $\tilde{\xi}(t)$, the density matrix $\tilde{\varrho}(t)$ of the system satisfies the stochastic Liouville-von Neumann equation, namely

$$\frac{\mathrm{d}}{\mathrm{d}t}\tilde{\varrho}(t) = -\frac{i\omega_0}{j}[J_z, \tilde{\varrho}(t)] - \frac{i\lambda_0}{j}\tilde{\xi}(t)[V, \tilde{\varrho}(t)]. \tag{8}$$

The limit $j \to \infty$ can be interpreted as a classical limit of the evolution equation [17]. In other words, the larger the j is, the more classical the system is, because its evolution can be effectively described as a classical dynamical system [9,17].

2.2 Going to a dimensionless form

We introduce the dimensionless time $s = \omega_0 t$ and transform Eq. (8) to the form

$$\frac{\mathrm{d}}{\mathrm{d}s}\varrho(s) = -\frac{i}{j}[J_z, \varrho(s)] - \frac{i\lambda}{j}\xi(s)[V, \varrho(s)]. \tag{9}$$

where

$$\varrho(s) = \tilde{\varrho}\left(\frac{s}{\omega_0}\right) = \tilde{\varrho}(t), \quad \lambda = \frac{\lambda_0}{\sqrt{\omega_0}} \tag{10}$$

and rescaled δ-correlated noise

$$\xi(s) = \frac{1}{\sqrt{\omega_0}}\tilde{\xi}\left(\frac{s}{\omega_0}\right) \tag{11}$$

has a zero mean value and the same intensity D_0 as $\tilde{\xi}(t)$ in Eq. (7). Instead of searching for a solution of Eq. (9), what is even for a white noise case a formidable task, we focus our attention on averaged quantum dynamics, i.e., on time evolution of the quantum state $\rho(s) = \langle\varrho(s)\rangle$, which can be interpreted in a similar fashion as one does in the case of reduced dynamics of open quantum systems [4]. The averaged dynamics of a noise-driven system in Eq. (9) is determined by the exact master equation in the dimensionless form [23,24]:

$$\frac{\mathrm{d}}{\mathrm{d}s}\rho(s) = -\frac{i}{j}[J_z, \rho(s)] - \frac{D}{j^2}[V, [V, \rho(s)]], \tag{12}$$

where $D = \lambda^2 D_0$ is the rescaled noise intensity (or equivalently the rescaled coupling strength). This equation is of the Lindblad form [2], and for any initial preparation, its solution $\rho : s \to \rho(s)$ is nonnegative [2]. It has been derived under the assumption that initial conditions for the system alone are imposed independently of the stochastic driving $\xi(t)$, i.e.,

$$\langle\xi(0)\rho(0)\rangle = \langle\xi(0)\rangle\rho(0) = 0. \tag{13}$$

It is worth noting that the master equation of a similar structure occurs for other models of reduced dynamics. We mention two of them: a general class of nondissipative continual measurements of an angular momentum [32] and exact dynamics of (1/2)-spin in contact with a quantum bosonic thermostat via the dephasing interaction [22].

2.3 Two-dimensional invariant subspace

In the following sections, we will use the notation:

$$|+\rangle = \frac{1}{\sqrt{2}}(|j, j\rangle + |j, -j\rangle) \tag{14}$$

$$|-\rangle = \frac{1}{\sqrt{2}}(|j, j\rangle - |j, -j\rangle) \tag{15}$$

for a linear combination of the J_z operator eigenstates with extreme eigenvalues $m = \pm j$ (for arbitrary $j > 0$). A subspace spanned by the basis vectors $\{|+\rangle, |-\rangle\}$ we denote as $\mathcal{H}_q = \text{span}(\{|+\rangle, |-\rangle\})$. It is clear that the states Eq. (14) and Eq. (15) transform under an action of the rescaled operator J_z/j as follows:

$$\begin{aligned} \frac{1}{j} J_z |+\rangle &= |-\rangle \\ \frac{1}{j} J_z |-\rangle &= |+\rangle \end{aligned} \tag{16}$$

and are orthonormal $\langle\alpha|\beta\rangle = \delta_{\alpha\beta}$ for $\alpha, \beta = 0, 1$. From the above rules, we can conclude that the subspace $\mathcal{H}_q$ is invariant under the action of a time evolution generated by J_z/j. It means that for an arbitrary large angular momentum j, one can always construct a subspace which behaves as a qubit system. The action of the operator J_z/j on the states $|+\rangle, |-\rangle$ is equivalent to the action of the σ_x operator on the canonical qubits states, i.e., eigenvectors of σ_z operator. In particular, it means that if a system is projected on one of these two states $|+\rangle, |-\rangle$, then after that a system starts to oscillate between them with frequency ω_0 (for $D = 0$).

3 Results

The Leggett–Garg scenario for testing realism requires a measurement of a dichotomous variable. We consider a projective measurement of a single observable Q of the form:

$$Q = \sum_{q=\pm 1} q \, \Pi_q \tag{17}$$

where

$$\Pi_+ = |+\rangle \langle +| \tag{18}$$

$$\Pi_- = \mathsf{I} - \Pi_+, \tag{19}$$

and I is the identity operator. In the following, we restrict our analysis to the three different dynamical scenarios in Eq. (12): the noise-free ($D = 0$), with the longitudinal coupling ($V = J_z$) and the transverse coupling ($V = J_x$). We present analytical solutions for a noise-free and longitudinal coupling for the initial states in the H_q subspace and perform a numerical simulations for the transverse coupling.

3.1 Noise-free system

Setting $D = 0$ in Eq. (12), for any initial state $|\psi\rangle \in \mathcal{H}_q$, the presented here scheme of a measurement and dynamics is equivalent to the widely studied system of the processing qubit. Taking it into consideration, we can immediately write down a form of the K_3 function, defined commonly for a fixed inter-measurement time interval τ (i.e., $s_3 - s_2 = s_2 - s_1 = \tau$):

$$K_3 = 2\cos(2\tau) - \cos(4\tau). \tag{20}$$

We want to stress that the definition of the states Eq. (14) and the following discussion is j-independent. Such a specific choice of the measurement as defined in Eq. (18) and Eq. (19) is particularly convenient since it allows to extract from the function K_3 the information related purely to the intensity D of noise $\xi(t)$. In other words, any modification of K_3 from the above form will be, for fixed V in Eq. (3), solely a noise-induced effect.

3.2 Longitudinal coupling

As we mentioned before, the action of the J_z/j operator on the states $\{|+\rangle, |-\rangle\}$ is equivalent to the action of a Pauli matrix σ_x on the canonical qubit states. Thus, if initial state belongs to the introduced invariant subspace, i.e., $|\psi\rangle \in H_q$, then Eq. (12) for $V = J_z$ can be reduced to the matrix form:

$$\frac{\mathrm{d}}{\mathrm{d}s}\rho(s) = -i[\sigma_x, \rho(s)] - D[\sigma_x, [\sigma_x, \rho(s)]], \tag{21}$$

where $\rho(s)$ is a matrix representation of a density operator in time s, computed in the basis $\{|+\rangle, |-\rangle\}$, and $\rho(0) = |\psi\rangle\langle\psi|$. We parameterized it as follows:

$$\rho(s) = \begin{bmatrix} p_+(s) & c(s) \\ c^*(s) & p_-(s) \end{bmatrix} \tag{22}$$

where $p_\pm = \mathrm{Tr}(\Pi_\pm \rho)$. Substituting Eq. (22) into Eq. (21), we obtain:

$$\frac{\mathrm{d}}{\mathrm{d}s}\rho(s) = \begin{bmatrix} -(r(s) + 2Dp(s)) & i(p(s) - 2Dr(s)) \\ -i(p(s) - 2Dr(s)) & r(s) + 2Dp(s) \end{bmatrix} \tag{23}$$

where $p \equiv p_+ - p_-$ and $r \equiv i(c^* - c)$. From the above, we can write down the equation of motion for real variables p and r in the matrix form:

$$\frac{\mathrm{d}}{\mathrm{d}s}\begin{bmatrix} p(s) \\ r(s) \end{bmatrix} = \begin{bmatrix} -4D & -2 \\ 2 & -4D \end{bmatrix}\begin{bmatrix} p(s) \\ r(s) \end{bmatrix}. \tag{24}$$

The general solution can be written as a superposition:

$$\begin{bmatrix} p(s) \\ r(s) \end{bmatrix} = Ae^{\lambda_1 s}\mathbf{v_1} + Be^{\lambda_2 s}\mathbf{v_2} \tag{25}$$

where the $\mathbf{v_i}$ and λ_i (for $i = 1, 2$) are, respectively, eigenvectors with associated eigenvalues of the generator of a differential equation Eq. (24). In this case, we have:

$$\begin{bmatrix} p(s) \\ r(s) \end{bmatrix} = Ae^{-4Ds-2is}\begin{bmatrix} 1 \\ i \end{bmatrix} + Be^{-4Ds+2is}\begin{bmatrix} 1 \\ -i \end{bmatrix}. \tag{26}$$

From this general solution, one can calculate the correlator K_3 for any initial state $|\psi\rangle \in H_q$, but in the following analysis, we will restrict our consideration to either a state $|+\rangle$ or $|-\rangle$. From this assumption, one can find out that $A = B = \pm\frac{1}{2}$. Since variables $p(s)$ and $r(s)$ are assumed to be real, from the above, we can extract two real solutions taking the real and imaginary part. Finally, we obtain:

$$\begin{bmatrix} p(s) \\ r(s) \end{bmatrix} = \pm e^{-4Ds}\begin{bmatrix} \cos(2s) \\ \sin(2s) \end{bmatrix}. \tag{27}$$

Next, we can define a conditional probability $p(q_2, s_2|q_1, s_1) \equiv p(q_2|q_1)$ of obtaining result $q_2 = \pm 1$ in time s_2 when in time s_1 was observed the value $q_1 = \pm 1$. Since $p_\pm(s) = \frac{1}{2}(1 \pm p(s))$, then we have:

$$p(q_2|q_1) = \frac{1}{2}\left[1 + (-1)^{\delta_{q_1 q_2}}|p(\Delta s)|\right] \tag{28}$$

where $\Delta s = s_2 - s_1$. From that, one can construct a two-time probability $p(q_2, s_2; q_1, s_1) \equiv p(q_2, q_1)$ of obtaining a value q_1 in time s_1 and a value q_2 in time s_2 as a product $p(q_2, q_1) = p(q_2|q_1)p_{q_1}$. From that, one can find out that correlation function Eq. (2) is equal:

$$C_{s_2 s_1} = \sum_{q_1, q_2 = \pm 1} q_1 q_2 \; p(q_2, q_1) = e^{-4D\Delta s}\cos(2\Delta s) \tag{29}$$

for a system initially prepared either in $|+\rangle$ state or $|-\rangle$ state. Finally, we conclude that K_3 function [Eq. (1)] for coupling $V = J_z$ and fixed inter-measurement is given by:

$$K_3 = e^{-4D\tau}\left(2\cos(2\tau) - e^{-4D\tau}\cos(4\tau)\right). \tag{30}$$

3.3 Transverse coupling

Analytical calculations performed for the longitudinal coupling $V = J_z$ are possible due to a dynamic invariance of the subspace spanned by $|\pm\rangle$ states. Unfortunately, for

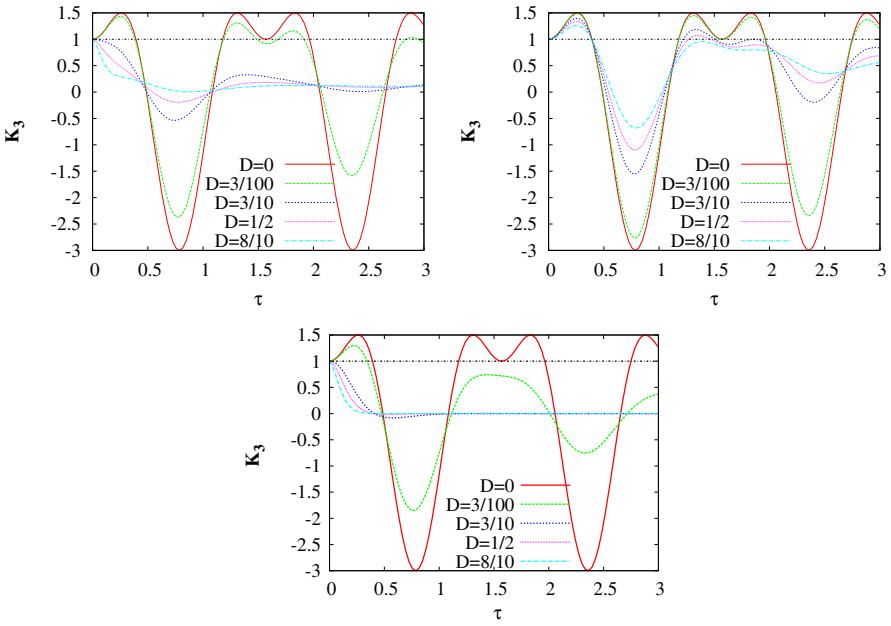

Fig. 1 The Leggett–Garg function K_3 versus inter-measurement time interval τ for selected values of the noise intensity D. *Top left panel* the quantum top with $j = 1$ and the coupling operator $V = J_x$. *Top right panel*: $j = 5$ and $V = J_x$. *Bottom panel* $V = J_z$ and arbitrary j number. Numerical data in all figures are prepared using QuTip, a Python-based computational toolbox [19] (Color figure online)

different types of coupling, it is no more the case. In particular, there is no method to solve analytically Eq. (12) for a coupling $V = J_x$. For such a transverse coupling, we perform numerical simulations using the Python-based toolbox QuTip [19] which is particularly useful for studying finite-dimensional open quantum systems described in terms of the Master Equations of a type Eq. (12), cf. Ref. [19] for details of the applied numerical procedure. In order to compare effectively two different types of coupling, the transverse with the longitudinal one, we restrict the analysis to a system initial preparation $\rho(0) = |+\rangle\langle+|$. The results are presented in Figs. 1 and 2.

4 Discussion

For the considered model, there are three elements affecting the LGI. The first, probably most natural, is the noise intensity D which occurs as the amplitude of the non-unitary part of the generator in Eq. (9). The second, more fundamental, is the way how external noise couples to the evolving quantum top encoded in the operator V in Eq. (3). The third, related to a semi-classical limit of the top evolution, is the size j of the top related to the dimension of the Hilbert space of the quantum system [3]. As presented in the last section, a solution of a noise-free system is j-independent; thus, it can be used as a natural reference to the noise-induced couplings. Furthermore, a longitudinal ($V = J_z$) coupling solution is also j-independent, and then, one can extract from this effects purely connected with the noise intensity D (or strength of a coupling λ). And

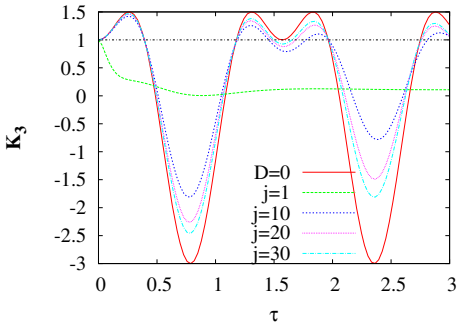

Fig. 2 The Leggett–Garg function K_3 versus inter-measurement time interval τ for the quantum top with different values of j. The noise intensity is $D = 0.8$ and the coupling operator is $V = J_x$ (Color figure online)

finally, a j-dependent solution for J_x coupling indicates how macrorealism is violated with respect to the dimension of a system state space. That is why we propose such specific form of the measured observable Eq. (17) and initial state $|\psi\rangle \in H_q$, since that model gives straightforward answers to all questions posed at the beginning. In addition, at the end we analyze the impact of a special scaling of the angular momentum operator $\mathbf{J}$ by a factor $1/j$ [Eq. (4)].

4.1 Impact of noise

Let us start analysis with the impact of the noise intensity D on time evolution and the resulting violation of the LGI in Eq. (1). For the noiseless case $D = 0$, the correlator K_3 is explicitly given by the formula in Eq. (20) and can serve as a reference function. With a gradual increase in D, the time evolution of the system becomes far from unitary and one expects that genuine quantum properties, such as the violation of LGI, become less detectable. This intuitive picture is confirmed by the analytical result Eq. (30) for longitudinal coupling, where we see that dumping of LGI correlator is of the exponential form. Examples of different forms of the K_3 function for $V = J_z$ with respect to noise intensity D are present in the bottom panel in Fig. 1. In addition, results from numerical simulations for transverse ($V = J_x$) coupling are presented in the upper panel in Fig. 1. In top left panel, the correlator K_3 for the system with the fixed quantum number $j = 1$ is depicted for several values of the noise intensity D. For weak noise ($D = 3/100$), the function K_3 represents weakly damped oscillations with several τ-intervals in which the LGI is violated. For strong noise (the case $D \geq 3/10$ in left panel), the impact of noise is decisive: One cannot detect the violation of the LGI. For larger values of the quantum number $j = 5$ (top left panel), the violation of the LGI can be observed for more numbers of windows of τ-intervals. Even for strong noise with $D = 8/10$, the LGI is violated and can be detected in one short τ-interval between successive measurements.

4.2 Role of coupling

Less intuitive is the influence of remaining two ingredients. Comparing plots in top left and bottom panels of Fig. 1 for the coupling via the operators J_x and J_z, respectively,

one concludes that for $V = J_z$ the effect of noise is stronger: For $D = 3/100$, the LGI is violated only in one window of the τ-interval, while for $V = J_x$, there are four τ-intervals in which the LGI is violated. We observe that in order to maintain the violation of LGI in a longer time for $V = J_z$, one needs the noise intensity to be much smaller than in the case when $V = J_x$. It might be considered as counterintuitive because in the case $V = J_z$, the quantum top effectively undergoes Markovian *pure dephasing* [4], i.e., $J_z(s) = J_z(0)$ is a constant of motion. It mimics an open quantum system with no energy exchange with the source of noise. In the case of seemingly stronger decoherence for $V = J_x$ and for a fixed noise intensity D, the LGI violation is weaker.

4.3 Dependence on the quantum number j

The effect of the size j of the top might also be counterintuitive. It seems that for large j, the system should be more classical, and in consequence, the LGI should be more robust. From Eq. (30), it is clear that for $V = J_z$ the correlator K_3 inherits j-independence recognized already in the noiseless case $D = 0$ [Eq. (20)]. Comparing curves in top left and top right panels in Fig. 1, one notices that the violation of the LGI is *more stable* with respect to noise for *larger* values of j. It is even more apparent in the semi-classical limit of large j as presented in Fig. 2: When j becomes larger and larger, the function K_3 becomes closer and closer to the noiseless case $D = 0$. In other words, for the semi-classical top, the violation of the LGI becomes more significant comparing to the top operating at the deep quantum regime of small j. The full analysis of how the maximum of K_3 changes with respect to j (for different noise intensity D) is presented in the upper panels of Fig. 3. From these, we see surprisingly that the maximal violation of LGI is non-monotonic in the whole domain, but it is only monotonically increasing for the values $j > 1$ and monotonically decreasing for $j < 1$ and relatively high values of noise intensity.

The reason of this phenomenon becomes apparent if one examines the trace distance $\Delta(s)$ between the noisy state $\rho(s)$ when $D > 0$ and the noiseless state $\rho_0(s)$ when $D = 0$. The trace distance is defined by the relation [30]

$$\Delta(s) = \frac{1}{2}\mathrm{Tr}\,|\rho(s) - \rho_0(s)|\,, \tag{31}$$

where $|X| = \sqrt{X^\dagger X}$ for any operator X. In Fig. 3, one can observe that at a fixed time instant s, the distance between the noisy state $\rho(s)$ and the noiseless state $\rho_0(s)$ decreases when the quantum number j increases. As the trace distance is a quantifier of *distinguishability* of states [30], we conclude that in the semi-classical limit $j \gg 1$ the noisy and noiseless evolution are more similar than in the case of quantum system with small values of j. This feature is responsible also for the behavior of the correlator K_3 and the violation of the Leggett–Garg realism.

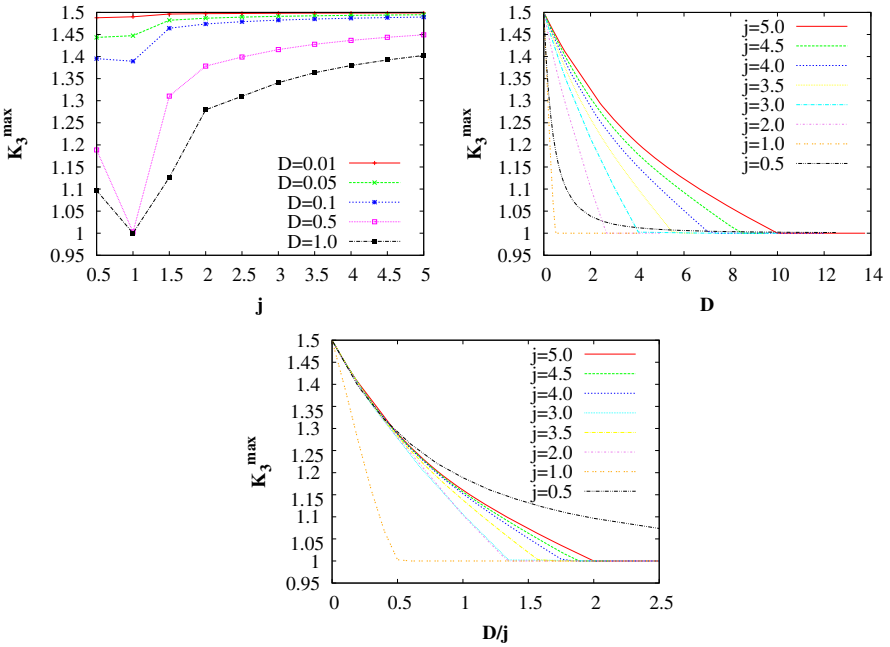

Fig. 3 The maximum of the Leggett–Garg function K_3 for the transverse coupling ($V = J_x$) versus: (*top left panel*) the absolute value of the quantum top angular momentum j with different values of a noise intensity D, (*top right panel*) the noise intensity D for different values of j and (*bottom panel*) the rescaled noise intensity D/j. Panel at the *bottom* is used as a reference, since it shows a maximum value of the K_3 function with respect to the noise intensity D/j, which is equivalent to the noise intensity D for a model without scaling $1/j$. It shows a little bit different behavior than in the rescaled model (*top right panel*), but they exhibits the same main feature that higher j values are more resistant on the applied noise. As it is seen from graphs, a scaling makes systems more distinguishable with respect to their angular momentum, especially systems violate Leggett–Garg inequalities differently for all values of a noise intensity, whereas in the non-rescaled model, we can distinguish between different j-states only in the regime of high D values. Interesting is a fact that a system with $j = 1$ is enormously low resistant on the noise (in both models) and system with $j = 1/2$ is enormously high resistant (in non-rescaled model) (Color figure online)

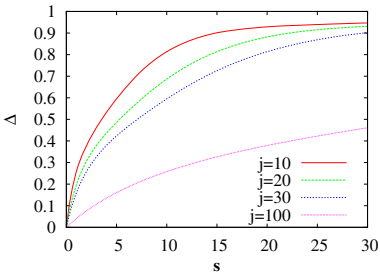

Fig. 4 Trace distance calculated between the noisy state $\rho(s)$ (for $D = 0.8$ and $V = J_x$) and noiseless state $\rho_0(s)$ ($D = 0$) for selected values of j (Color figure online)

4.4 Role of scaling

At the end, we present how the special scaling of the angular momentum **J** operator by a factor $1/j$ in Eq. (4) (which we use in order to analyze a semi-classical behavior)

affects a violation of the Leggett–Garg inequalities. Let us notice a very different physical content of both the scaled and non-scaled models. The first describes a well-defined semi-classical limit of a well-established quantum system, whereas the second is an essentially quantum system described by quantum numbers of a relatively large values.

As it can be inferred from Eq. (12), a model without scaling can be restored by the replacement: $s \to js$ and $D \to jD$, which transform Eq. (30) into the relation:

$$K_3 = e^{-4Dj^2\tau}\left(2\cos(2j\tau) - e^{-4Dj^2\tau}\cos(4j\tau)\right). \tag{32}$$

In this case, we observe a strong dumping of the K_3 function amplitude for the systems with higher angular momentum j. In addition, without scaling, a period of K_3 function is also affected by the total angular momentum of the system. We want to stress that the j-independent solution for the operators Eq. (4) has a source in the special action of the operator J_z/j on the states $|+\rangle$, $|-\rangle$ in Eq. (16).

We also analyze an impact of scaling at the maximum of the K_3 amplitude with respect to j number for a transverse coupling. For this reason, we present the results for non-rescaled model in the bottom panel in Fig. 4. Surprisingly, we observe very similar behavior like in main (scaled) model in this paper, i.e., systems with higher angular momentum j are more resistant with respect to noise in the context of violation of the macrorealism. It is an opposite behavior if one compares it with the J_z coupling for non-scaled model [Eq. (32)].

5 Conclusions

Realism of classical objects seems to be unquestionable. Almost no one doubts that 'there is a moon when nobody looks' [28]. The case of a 'flux' [21] is less obvious, whereas for microscopic objects, the violation of Leggett–Garg realism is probably as generic as the violation of local realism of composite systems [18].

In this work, we study the quantum top assisted by classical Gaussian white noise starting from a very quantum regime of small values of the quantum number j and finishing in the semi-classical regime of large j. We investigate the violation of the LGI involving the function K_3 in Eq. (1). The measurement defined in Eq. (18) is chosen in such a way that in the absence of noisy driving, the correlator K_3 is j-independent. We consider two types of coupling V in Eq. (3). For $V = J_z$, the function K_3 is shown to be j-independent, although the LG inequality is, in the presence of noise, less likely violated. For $V = J_x$, the violation of the LG inequality is more stable than in the case $V = J_z$. We observe that for $V = J_x$ the violation still occurs but for the noise intensity larger than in the case $V = J_z$. In other words, for a given amount of noise in the system and the coupling $V = J_x$, the Leggett–Garg realism is 'better violated' than in the case $V = J_z$. Moreover, contrary to a natural intuition, the semi-classical noise-assisted top is, for a given amount of noise and $V = J_x$, more likely to be a stage of the violation of the Leggett–Garg realism.

We hope that despite simplicity of the considered model, results of the paper enhance our understanding of what Leggett–Garg realism is and how it can be controlled by external stochastic driving.

Acknowledgments The work has been supported by the NCN project DEC-2013/09/B/ST3/01659 (JD).

References

1. Accardi, L., Lu, Y., Volovich, I.: Quantum Theory and its Stochastic Limit. Springer, Berlin (2002)
2. Alicki, R., Lendi, K.: Quantum Dynamical Semigroups and Applications. Lecture Notes in Physics. Springer, Berlin (2007)
3. Biedenharn, L., Louck, J.: Angular Momentum in Quantum Physics. Theory and Application. Cambridge University Press, Cambridge (1984)
4. Breuer, H.P., Petruccione, F.: The Theory of Open Quantum Systems. Oxford University Press, Oxford (2003)
5. Brunner, N., Cavalcanti, D., Pironio, S., Scarani, V., Wehner, S.: Bell nonlocality. Rev. Mod. Phys. **86**, 419–478 (2014). doi:10.1103/RevModPhys.86.419
6. Budroni, C., Emary, C.: Temporal quantum correlations and leggett-garg inequalities in multilevel systems. Phys. Rev. Lett. **113**, 050,401 (2014). doi:10.1103/PhysRevLett.113.050401
7. Dajka, J.: Disentanglement of qubits in classical limit of interaction. Int. J. Theor. Phys. **53**(3), 870–880 (2014). doi:10.1007/s10773-013-1876-9
8. D'Alessandro, D.: Introduction to Quantum Control and Dynamics. Taylor & Francis Group, London (2008)
9. Demkowicz-Dobrzański, R., Kuś, M.: Global entangling properties of the coupled kicked tops. Phys. Rev. E **70**, 066,216 (2004). doi:10.1103/PhysRevE.70.066216
10. Elze, H.T.: Linear dynamics of quantum-classical hybrids. Phys. Rev. A **85**, 052,109 (2012). doi:10.1103/PhysRevA.85.052109
11. Emary, C.: Decoherence and maximal violations of the leggett-garg inequality. Phys. Rev. A **87**, 032,106 (2013). doi:10.1103/PhysRevA.87.032106
12. Emary, C., Lambert, N., Nori, F.: Leggett–garg inequalities. Rep. Prog. Phys. **77**(1), 016,001 (2014). http://stacks.iop.org/0034-4885/77/i=1/a=016001
13. Fratino, L., Lampo, A., Elze, H.T.: Entanglement dynamics in a quantum–classical hybrid of two q-bits and one oscillator. Phys. Scr. **2014**(T163), 014,005 (2014). http://stacks.iop.org/1402-4896/2014/i=T163/a=014005
14. Gardiner, C.: Handbook of Stochastic Methods. Springer, Berlin (1997)
15. Gühne, O., Tóth, G.: Entanglement detection. Phys. Rep. **474**(1–6), 1–75 (2009). doi:10.1016/j.physrep.2009.02.004. http://www.sciencedirect.com/science/article/pii/S0370157309000623
16. Gihman, I., Skorohod, A.V.: Controlled Stochastic Processes. Springer, Berlin (1979)
17. Haake, F.: Quantum Signatures of Chaos. Wiley, Hoboken (1991)
18. Horodecki, R., Horodecki, P., Horodecki, M., Horodecki, K.: Quantum entanglement. Rev. Mod. Phys. **81**, 865–942 (2009). doi:10.1103/RevModPhys.81.865
19. Johansson, J., Nation, P., Nori, F.: Qutip 2: a python framework for the dynamics of open quantum systems. Comp. Phys. Commun. **184**(4), 1234–1240 (2013). doi:10.1016/j.cpc.2012.11.019. http://www.sciencedirect.com/science/article/pii/S0010465512003955
20. Lampo, A., Fratino, L., Elze, H.T.: Mirror-induced decoherence in hybrid quantum-classical theory. Phys. Rev. A **90**, 042,120 (2014). doi:10.1103/PhysRevA.90.042120
21. Leggett, A.J., Garg, A.: Quantum mechanics versus macroscopic realism: Is the flux there when nobody looks? Phys. Rev. Lett. **54**, 857–860 (1985). doi:10.1103/PhysRevLett.54.857
22. Łuczka, J.: Spin in contact with thermostat: exact reduced dynamics. Phys. A **167**, 919 (1990). doi:10.1016/0378-4371(90)90299-8

23. Łuczka, J.: Quantum open systems in a two-state stochastic reservoir. Czech. J. Phys. **41**(17), 289 (1991)
24. Łuczka, J., Niemiec, M.: A master equation for quantum systems driven by poisson white noise. J. Phys. A Math. Gen. **24**(17), L1021 (1991). http://stacks.iop.org/0305-4470/24/i=17/a=010
25. Mahler, G., Weberruss, V.: Quantum Networks. Dynamics of Open Nanostructures. Springer, Berlin (1998)
26. Markiewicz, M., Kurzyński, P., Thompson, J., Lee, S.Y., Soeda, A., Paterek, T., Kaszlikowski, D.: Unified approach to contextuality, nonlocality, and temporal correlations. Phys. Rev. A **89**, 042,109 (2014). doi:10.1103/PhysRevA.89.042109
27. Maroney, O.J.E., Thomson, C.G.: Quantum- vs. macro- realism: What does the leggett-garg inequality actually test? (2014). arXiv:1412.6139
28. Mermin, N.D.: Is the moon there when nobody looks? Reality and the quantum theory. Phys. Today **38**(4), 38–47 (1985)
29. Modi, K., Brodutch, A., Cable, H., Paterek, T., Vedral, V.: The classical-quantum boundary for correlations: Discord and related measures. Rev. Mod. Phys. **84**, 1655–1707 (2012). doi:10.1103/RevModPhys.84.1655
30. Nielsen, M., Chuang, I.: Quantum Computation and Quantum Information. Cambridge University Press, Cambridge (2000)
31. Perelomov, A.: Generalized Coherent States and Their Applications. Springer, Berlin (1986)
32. Sanders, B.C.: Quantum dynamics of the nonlinear rotator and the effects of continual spin measurement. Phys. Rev. A **40**, 2417–2427 (1989)
33. Wang, X., Ma, J., Song, L., Zhang, X., Wang, X.: Spin squeezing, negative correlations, and concurrence in the quantum kicked top model. Phys. Rev. E **82**, 056,205 (2010). doi:10.1103/PhysRevE.82.056205
34. Wiesman, H., Milburn, G.: Quantum Measurement and Control. Cambridge University Press, Cambridge (2009)